# Photodissociation Dynamics of Organometallics: Quantum Simulation for the Dihydride Complex $H_2Fe(CO)_4$

## Marie-Catherine Heitz* and Chantal Daniel*

*Contribution from the Laboratoire de Chimie Quantique UPR 139 du CNRS, Institut Le Bel, 4 rue Blaise Pascal, 67000 Strasbourg, France*

*Received December 16, 1996. Revised Manuscript Received May 13, 1997*[⊗]

**Abstract:** The photodissociation dynamics of $H_2Fe(CO)_4$ have been studied through wave packet propagations on CASSCF/CCI potentials, calculated for the electronic ground and excited states, as a function of two coordinates $q_a$ and $q_b$ corresponding to molecular hydrogen elimination and CO dissociation, respectively. The theoretical absorption spectrum is characterized by two bands at 272 nm (36 700 cm$^{-1}$) and 246 nm (40 500 cm$^{-1}$) which have been assigned to the $a^1A_1 \rightarrow a^1B_1$ and $a^1A_1 \rightarrow b^1A_1$ transitions, respectively. The first band corresponds to the experimental maximum observed around 270 nm. A semiquantitative mechanism has been proposed for the photodissociation of the title molecule: (i) under irradiation at 254 nm, the $a^1B_1$ ($3d_{yz} \rightarrow \sigma_g^*$) and $b^1A_1$ ($3d_{x^2-y^2} \rightarrow \sigma_g^*$) excited states will be populated; (ii) from the $b^1A_1$ state, the molecule will dissociate in a total and ultrafast (less than 40 fs) reaction toward the formation of $Fe(CO)_4$ and molecular hydrogen; (iii) after the initial $a^1A_1 \rightarrow a^1B_1$ transition, the reactive system will evolve into two competitive channels, leading mainly to the elimination of $H_2$ in a very short time scale (40 fs) and as second minor primary reaction (4%) toward the CO dissociation in 100 fs. The nonradiationless transitions to the low-lying triplet states occur in a picosecond time scale and have a rather low probability indicating the minor role of the triplet states at the early stage of the photodissociation.

## 1. Introduction

The photochemical reaction currently observed after irradiation of transition metal di- and polyhydrides is the reductive elimination of molecular hydrogen

$$H_2ML_x \xrightarrow{h\nu} H_2 + ML_x \qquad (1)$$
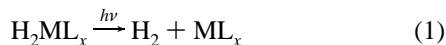
leading to highly reactive intermediates which are able to activate the carbon−hydrogen bonds in saturated organic compounds.[1−7] Flash photolysis experiments have led to the conclusion that there are at least two mechanisms operative for the photoelimination of $H_2$ from dihydride complexes: one being the concerted loss of $H_2$ from the initial molecule, the other being the prior dissociation of another ligand to give an unsaturated intermediate that undergoes rapid elimination of molecular hydrogen.[8,9] Despite of the very intense activity developed in this field in the past ten years, even enhanced by the discovery of the so-called nonclassical hydride complexes,[10−13] many fundamental questions remain unsolved: (i) the factors governing the mechanism of reaction (1); (ii) the efficiency of the corresponding reverse reaction, namely the oxidative addition; (iii) the occurrence of concurrent primary reactions; (iv)

the excited states dynamics; and (v) the branching ratio between dissociative and nondissociative pathways. The laser experiments, reported for this class of molecules and performed either in low-temperature matrices or in solution, are mainly oriented toward the determination of intermediates or toward the kinetics and the efficiency of the carbon−hydrogen bond activation. Recent flash photolysis experiments supported by careful IR spectroscopy have shown that, regarding the multiplicity of channels available in the UV−visible region due to the high density of excited states, the behavior of the molecule depends strongly on the metal center, the ligands, and the experimental conditions. This complexity is illustrated by the photochemistry in solution of $H_2IrCl(L')(PPh_3)_2$ ($L' = CO$ or $PPh_3$) and $H_2$-$RhCl(PPh_3)_3$ dihydrides. A ligand dissociation to give a five-coordinate intermediate $H_2MCl(PPh_3)_2$ which undergoes rapid elimination of $H_2$ competitive with back reaction with $L'$ is proposed for the iridium complex, while a concerted dihydrogen elimination to give $MCl(PPh_3)_3$ as the primary product operates for the rhodium analog.[9] More recent matrix isolation studies reported for metal hydride complexes of the series Fe, Ru, and Os have demonstrated that 16-electron fragments can be produced by photolysis of the dihydride precursors $M(dmpe)_2H_2$ ($M = Fe$, Ru).[14,15] The iron and ruthenium fragments exhibit a remarkable difference in reactivity toward the C−H activation. Kinetic investigations with laser flash photolysis have shown that $Ru(dmpe)_2$ reacts over $10^4$ times more rapidly with $H_2$ than does $Fe(dmpe)_2$. When present in the coordination sphere, the loss of a carbonyl ligand is competitive with the molecular hydrogen elimination. The lone exceptions are $H_2Fe(CO)_4$ (reaction 2) and $H_2IrCp(CO)$, which eliminate specifically $H_2$

⊗ Abstract published in *Advance ACS Abstracts,* July 15, 1997.
(1) Janowiz, A. H.; Bergman, R. G. *J. Am. Chem. Soc.* **1982**, *104*, 352; **1983**, *105*, 3929.
(2) Wenzel, T. J.; Bergman, R. G. *J. Am. Chem. Soc.* **1986**, *108*, 4856.
(3) Fisher, B. J.; Eisenberg, R. *Organometallics* **1983**, *2*, 764.
(4) Wu, J.; Bergman, R. G. *J. Am. Chem. Soc.* **1989**, *111*, 7628.
(5) Peerlans, R. A.; Bergman, R. G. *Organometallics* **1984**, *3*, 508.
(6) Wax, M. J.; Strykler, J. M.; Buchanan, J. M.; Kovac, C. A.; Bergman, R. G. *J. Am. Chem. Soc.* **1984**, *106*, 1121.
(7) Jones, W. D.; Feher, F. J. *J. Am. Chem. Soc.* **1982**, *104*, 4240.
(8) Wink, D. A.; Ford, P. C. *J. Am. Chem. Soc.* **1985**, *107* ,5566.
(9) Wink, D. A.; Ford, P. C. *J. Am. Chem. Soc.* **1986**, *108* ,4838.
(10) Kubas, G. J.; Ryan, R. R.; Swanson, B. I.; Vergamini, P. J.; Wasserman, H. J. *J. Am. Chem. Soc.* **1984**, *100*, 451.
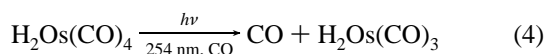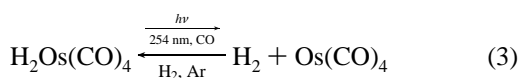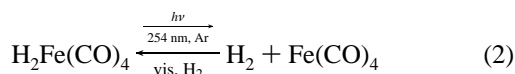(11) Kubas, G. J. *Acc. Chem. Res.* **1988**, *21*, 120.
(12) Crabtree, R. H.; Hamilton, D. G. *Adv. Organomet. Chem.* **1988**, *28*, 299.
(13) Crabtree, R. H. *Acc. Chem. Res.* **1990**, *23*, 95.

(14) Hall, C.; Jones, W. D.; Mawby, R. J.; Osmam, R.; Perutz, R. N.; Whitlesey, M. K. *J. Am. Chem. Soc.* **1992**, *114*, 7425. Whittlesey, M. K.; Mawby, R. J.; Osmam, R.; Perutz, R. N.; Field, L. D.; Wilkinson, M. P.; George, M. W. *J. Am. Chem. Soc.* **1993**, *115*, 8627.
(15) Mawby, R.; Perutz, R. N.; Whittlesey, M. K. *Organometallics* **1995**, *14*, 3268. Cronin, L.; Nicasio, M. C.; Perutz, R. N.; Peters, R. G.; Roddick, D. M.; Whittlesey, M. K. *J. Am. Chem. Soc.* **1995**, *117*, 10047.

upon photolysis.[16,17] For instance, upon irradiation under similar experimental conditions, the osmium analog to $H_2Fe(CO)_4$ behaves differently, leading both primary products $H_2Os(CO)_3$ and $Os(CO)_4$[18] (reactions 3 and 4)

$$H_2Fe(CO)_4 \xrightleftharpoons[\text{vis, } H_2]{\overset{h\nu}{254 \text{ nm, Ar}}} H_2 + Fe(CO)_4 \qquad (2)$$

$$H_2Os(CO)_4 \xrightleftharpoons[H_2, Ar]{\overset{h\nu}{254 \text{ nm, CO}}} H_2 + Os(CO)_4 \qquad (3)$$

$$H_2Os(CO)_4 \xrightarrow[254 \text{ nm, CO}]{h\nu} CO + H_2Os(CO)_3 \qquad (4)$$

Most of the recent theoretical work published in the field of transition metal hydrides is dedicated to structural problems (classical vs nonclassical hydrides) or to secondary reactions mechanisms.[20−23] Despite of the emergence of efficient modern quantum chemical methods able to treat the excited states in transition metal complexes,[24,25] little is known about the excited states reactivity. Current understanding of photochemical reactions is generally based on molecular orbital diagrams coupled with an analysis in terms of the bonding and antibonding character. The aim of a qualitative theoretical study, based on the potential energy surfaces (PES) which connect the ground and excited states of the reactant to those of the primary products, is to elucidate the mechanism of the primary process and to identify the photoactive excited states responsible for the photoreactivity of the molecule.[26−28] Understanding the occurrence of concurrent reactions (ligand loss vs radical formation or ligand loss vs elimination of $H_2$) represents a fundamental goal in a semiquantitative study of the photochemistry of organometallics. The ultimate purpose is the calculation of the branching ratio for the different pathways and the determination of the main features of the absorption spectra[29] through the simulation of the excited states dynamics.

Potential energy curves, based on CASSCF/CCI calculations, have been reported for the photoelimination of $H_2$ from $H_2Fe$-
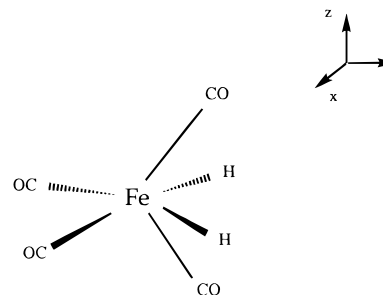
(16) Sweany, R. L. *J. Am. Chem. Soc.* **1981**, *103* , 2410.
(17) Bloyce, P. E.; Rest, A. J.; Whitwell, I.; Graham, W. A. G.; Holmas-Smith, R. J. *J. Chem. Soc., Chem. Commun.* **1988**, 846. Bloyce, P. E. ; Rest, A. J.; Whitwell, I. *J. Chem. Soc., Dalton Trans.* **1990**, 813.
(18) Rest, A. J. unpublished work referenced by Evans, J. and Norton, J. R.[19] Sweany, R. L. To be published.
(19) Evans, J.; Norton, J. R. *J. Am. Chem. Soc.* **1974**, *96*, 7577.
(20) Lin, Z.; Hall, M. B. *J. Am. Chem. Soc.* **1994**, *116*, 4446. Lin, Z.; Hall, M. B. *Organometallics*, **1993**, *12*, 4046. Haynes, G. R.; Martin, R. L.; Hay, P. J. *J. Am. Chem. Soc.* **1992**, *114*, 28. Ross, J. L.; Dickson, M.; Ziegler, T. *J. Am. Chem. Soc.* **1995**, *117*, 11482 and references therein.
(21) Kubas, G. J.; Barus, C. J.; Eckert, J.; Johnson, S. W.; Larson, A. C.; Vergamini, P. J.; Unkefer, C. J.; Khalsa, G. R. K.; Jackson, S. A.; Eisenstein, O. *J. Am. Chem. Soc.* **1993**, *115*, 569. Gusaev, D. G.; Kuhlman, R.; Sin, G.; Eisenstein, O.; Caulton, K. G. *J. Am. Chem. Soc.* **1994**, *116*, 2685. Maseras, F.; Duran, M.; Lledos, A.; Bertran, J. *J. Am. Chem. Soc.* **1991**, *113*, 2879.
(22) Ziegler, T.; Tschinke, V.; Liangyou, F.; Becke, A. D. *J. Am. Chem. Soc.* **1995**, *117*, 799. Siegbahn, P. E. M.; Svenson, M. *J. Am. Chem. Soc.* **1994**, *116*, 10124. Jimenez-Catano, R.; Hall, M. B. *Organometallics* **1996**, *15*, 1889.
(23) *Transition Metal Hydrides*; Dedieu, A.; Ed.; VCH Publishers, Inc. New York, 1991.
(24) Pierloot, K.; Van Praet, E.; Vanquickenborne, L. G.; Roos, B. O. *J. Phys. Chem.* **1993**, *97*, 12220. Persson, B. J.; Roos, B. O.; Pierloot, K. *J. Chem. Phys.* **1994**, *101*, 6810.
(25) (a) Heitz, M. C.; Daniel, C. *Chem. Phys. Lett.* **1995**, *246*, 488. (b) Guillaumont, D.; Daniel, C.; Vlcek, A., Jr. *Inorg. Chem.* **1997**, *36*, 1684.
(26) Veillard, A.; Strich, A. *J. Am. Chem. Soc.* **1988**, *110*, 3793.
(27) Daniel, C. *J. Am. Chem. Soc.* **1992**, *114*, 1625. Daniel, C. *Coord. Chem. Rev.* **1990**, *97*, 141.
(28) Daniel, C. *J. Phys. Chem.* **1991**, *95*, 2394.
(29) Daniel, C.; Heitz, M. C.; Lehr, L. Schröder, T.; Warmuth, B. *Int. J. Quant. Chem.* **1994**, *52*(7), 71. Daniel, C.; Kolba, E.; Lehr, L.; Schröder, T.; Manz, J. *J. Phys. Chem.* **1994**, *98*, 9823; Daniel, C.; Heitz, M. C.; Lehr, L.; Manz, J.; Schröder, T. *J. Phys. Chem.* **1993**, *97*(48), 12485.



**Figure 1.** Structure of $H_2Fe(CO)_4$ from ref 31.

**Scheme 1**



$(CO)_4$ reaction (2).[28] The qualitative mechanism proposed for this reaction states with excitation into one of the low-lying singlet excited states followed by intersystem crossing to the $a^3B_2$ state (corresponding to a $3d \rightarrow \sigma_u*$ excitation) ($\sigma_g$ and $\sigma_u$ are the bonding and antibonding configurations of the two hydrogen s orbitals which are metal−hydrogen bonding, $\sigma_g*$ and $\sigma_u*$ being similarly defined but metal−hydrogen antibonding (Scheme 1) and dissociation to the primary products $H_2 + Fe(CO)_4$ along the $a^3B_2$ curve. This potential energy curve corresponds in its dissociative part to a $\sigma_u \rightarrow \sigma_g*$ excitation, namely to the excitation of an electron from a MO which is H−H antibonding and M−H bonding to a MO which is H−H bonding and M−H antibonding. This mechanism describing the photoelimination of $H_2$ has been generalized to other transition metal di and polyhydrides.[30]

The aim of the present study is to present a complete quantum chemical study of the photodissociation of the title molecule, including an hypothetical dissociation of a carbonyl ligand,

$$H_2Fe(CO)_4 \xrightarrow[?]{h\nu} CO + H_2Fe(CO)_3 \qquad (5)$$
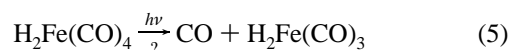
primary reaction which is observed under irradiation of the osmium analog $H_2Os(CO)_4$ (reaction 4). This numerical simulation is based on the two-dimensional potential energy surfaces calculated for the ground state and the lowest excited states as a function of the Fe−CO and Fe−$H_2$ elongations. The photodissociation dynamics is investigated by wavepacket propagations on these PES.

## 2. Computational Method

**Quantum Chemical Calculations.** The calculations were carried out starting from the experimental geometry of $H_2Fe$-$(CO)_4$ ($C_{2v}$ symmetry with $O_y$ the $C_2$ axis)[31] (Figure 1). Since the primary product of reaction 2, $Fe(CO)_4$ also has the $C_{2v}$ symmetry in its ground state $^3B_2$,[32] it was assumed that the $C_{2v}$ symmetry is retained along the reaction path corresponding to $H_2$ elimination (Scheme 2). According to gradient SCF calculations of the structure of $H_2Fe(CO)_3$,[33] primary product of the carbonyl dissociation, the reaction path corresponding to this other reaction should be described by the dissociation of an "axial" carbonyl under the $C_s$ symmetry constrained (Scheme

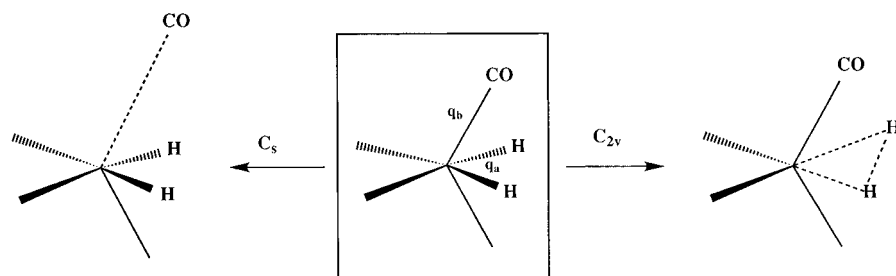(30) Veillard, A. *Chem. Phys. Lett.* **1990**, *170* (5,6), 441.
(31) McNeil, E. A.; Schöler, F. R. *J. Am. Chem. Soc.* **1977**, *99*, 6243.
(32) (a) Poliakoff, M.; Turner, J. J. *J. Chem. Soc., Dalton Trans* **1974**, 2276. (b) Daniel, C.; Bénard, M.; Dedieu, A.; Wiest, R.; Veillard, A. *J. Phys. Chem.* **1984**, *21*, 4805.
(33) Daniel, C. Unpublished.

**Scheme 2**



2). The symmetry constraints should not operate dramatically on the smooth profile of the excited potential energy surfaces which govern the mechanism of photochemical reactions. These assumptions are based on the fact that the symmetry restrictions usually affect the energy profiles characterized by high energy barriers.[34]

The two-dimensional PES $V(q_a,q_b)$ (with $q_a = [Fe-H_2]$ and $q_b = [Fe-CO]$), calculated under the $C_s$ symmetry constraint, have been obtained through complete active space SCF (CASS-CF)[35] calculations supplemented by a Configuration Interaction treatment. The CASSCF wave functions are used as references for the contracted configuration interaction (CCI) calculations.[36] Since our interest centers mostly on the lowest excited states of $H_2Fe(CO)_4$ corresponding to the $3d \rightarrow \sigma_g^*$, $3d \rightarrow \sigma_u^*$, and $\sigma_u \rightarrow \sigma_g^*$, the two orbitals involved in the bonding of the hydrogen ($\sigma_g$, $\sigma_u$) and their antibonding counterparts ($\sigma_g^*$, $\sigma_u^*$), the 3d orbitals and the d orbitals which correlate them were included in the active space of the CASSCF. Ten electrons were correlated in ten active orbitals in this 10e10a calculation. The CASSCF calculations were carried out for the lowest $^5A_2$ high spin state of main configuration $(\sigma_g)^2(\sigma_u)^2(3d_{xz})^2(3d_{yz})^1(3d_{x^2-y^2})^1(\sigma_g^*)^1(\sigma_u^*)^1$ which assures a balanced description of the different excited states.[38] For each electronic state, two CCI calculations were performed: the first one with one reference configuration corresponding to the required state, the second one being a multireference calculation including all the configurations that appear with a coefficient larger than 0.08 in the first monoreference CI wave function. Ten electrons are correlated and single and double excitations to all virtual orbitals, except the counterparts of the carbonyls 1s and of the metal 1s, 2s, and 2p orbitals, are included in the CCI calculation. The following basis sets were used: for the metal center a (15,11,6) set contracted to [9,6,3],[39] for the first-row atoms a (10,6) set contracted to [4,2],[42] and for hydrogen a (6,1) set contracted to

[3,1].[43] The excitation energies to the lowest excited states involved in the photodissociation of $H_2Fe(CO)_4$ and contributing to the absorption spectrum calculated through this approach have been compared to CASSCF/CASPT2 excitation energies obtained on the basis of CASSCF wave functions performed for each electronic state, using atomic natural orbitals (ANO) basis sets.[44] From this recent study,[25a] we have concluded that the present approach based on CCI calculations performed on top of a unique CASSCF wave function gives reasonable excitation energies as long as the reference wave function is judiciously chosen. This approach represents the best compromise for the calculation of excited states and corresponding PES, regarding the complexity of avoided crossing regions for which a CASPT2 treatment could be rather tricky.

The integral calculations were carried out either with the system of programs ARGOS[45] or with the system of programs ASTERIX.[37] The CCI calculations were performed with the program developed originally by Siegbahn using a multireference CI method[36] and the CASPT2 calculations with the MOLCAS-3 quantum chemistry software.[46] The dynamics has been simulated with the QMPRO program developed originally in Berlin.[47]

**Spin-Orbit Interaction.** The spin-orbit interaction between the singlet and triplet excited states has been evaluated using the effective one-electron operator[48]

$$H_{so}^{eff} = \sum_i A^{(i)} \cdot S^{(i)}, \quad A^{(i)} = \frac{\alpha}{2} \frac{Z_{eff}^{k,l}}{r_{k,i}^3}(r_{k,i}, p_i) \qquad (1)$$

where $Z_{eff}^{k,l}$ expresses the one center valence shell character. $k$ is the heavy atom center and $l$ is the valence shell azimuthal quantum number. This effective operator operates only on the 3d orbitals $l = 2$ and $k =$ Fe. $\alpha$ is the fine structure, $\langle r^{-3} \rangle$ is the expansion value from tables of ref 49 and $r_{k,i}$ is the one-electron nucleus distance. On the basis of a restricted full CI scheme,[50] the spin-orbit matrix (up to 400 000 determinants) is diagonalized to get the spin-orbit coupled excited states.[51]

**Simulation of the Dynamics.** For the sake of simplicity, the molecule is modeled as pseudotriatomic with two noncol-

(34) (a) Jaffe, R. L.; Hayes, M. M.; Morokuma K. *J. Chem. Phys.* **1974**, *60*(12), 5108. (b) Goddard, J. D.; Yamagushi, Y.; Schaefer III, H. F. *J. Chem. Phys.* **1981**, *75*(7), 3459. Goddard, J. D.; Schaefer III, H. F. *J. Chem. Phys.* **1979**, *70*(11), 5117.

(35) Siegbahn, P. E. M.; Almlöf, J.;Heiberg, A.; Roos, B. O. *J. Chem. Phys.* **1981**, *74*, 2384.

(36) Siegbahn, P. E. M.; *Int. J. Quantum. Chem.* **1983**, *23*, 1869. The original program was interfaced for use in conjunction with the Asterix system of programs on the CRAY's[37] by Daniel, C.; Speri, M.; Rohmer, M. M.

(37) Ernenwein, R.; Rohmer, M. M.; Bénard, M. *Comput. Phys. Comm.* **1990**, *58*, 305. Rohmer, M. M.; Demuynck, J.; Bénard, M.; Wiest, R.; Bachmann, C.; Henriet, C.; Ernenwein, R. *Comput. Phys. Comm.* **1990**, *60*, 127. Wiest, R.; Demuynck, J.; Bénard, M.; Rohmer, M. M; Ernenwein, R. *Comp. Phys. Comm.* **1991**, *62*, 107.

(38) Daniel, C.; Veillard, A. In *Transition Metal Hydrides*; VCH Publishers: Dedieu, A., Ed.; 1991; pp 235−261.

(39) This basis set is made from the (14.9.5) basis of Wachters[40] by adding an additional s function (exponent 0.3218), two diffuse p functions, and one diffuse d function. All the exponents were chosen according to the even-tempered criterion of Raffenetti.[41]

(40) Wachters, A. J. H. *J. Chem. Phys.* **1970**, *52*, 1033.

(41) Raffenetti, R. C.; Bardo, R. D.; Ruedenberg, K. in *Energy Structure and Reactivity,* Smith, D. W., McRae, W. B., Eds.; Wiley: New York, 1973; p 164.

(42) Huzinaga, S. *Approximate Atomic Functions: Technical Report*; University of Alberta: Alberta, 1971.

(43) Huzinaga, S. *J. Chem. Phys.* **1965**, *42*, 1293.

(44) Pierloot, K.; Dumez, B.; Widmark, P. O.; Roos, B. O. *Theor. Chim. Acta* **1995**, *90*, 87.

(45) Pitzer, R. *J. Chem. Phys.* **1973**, *58*, 3111.

(46) Andersson, K.; Blomberg, M. R. A.; Fülscher, M. P.; Karlström, G.; Kello, V.; Lindh, R.; Malmqvist, P. Å.; Noga, J.; Olsen, J.; Roos, B. O.; Sadlej, A. J.; Siegbahn, P. E. M.; Urban, M.; Widmark, P. O. Molcas-3; University of Lund: Sweden.

(47) Schmidt, B. QMPRO; Freie Universität: Berlin, Germany.

(48) Ribbing, C.; Odelius, M.; Laarksonen, A.; Kowalewski, J.; Roos, B. O. *Int. J. Quant. Chem. Quant. Chem. Symp.* **1990**, *24*, 295.

(49) Fischer, I. F. *The Hartree-Fock Method for Atoms (A numerical Approach)*; Wiley-Interscience, New York, 1977.

(50) Olsen, J.; Roos, B. O.; Jörgensen, P.; Aa Jensen, H. J. *J. Chem. Phys.* **1988**, *189*, 2185.

(51) Ribbing, C.; Daniel, C. *J. Chem. Phys.* **1994**, *100*, 6591.

linear dissociative bonds, $q_a = [Fe-H_2]$ and $q_b = [Fe-CO]$ (Scheme 2). All other "spectators" modes are decoupled in this zero-order approximation. This decoupling mode should be reasonable, at least for ultrafast time scales (of the order of 100 fs) when the initial energy remains in the dissociative bonds.

The photoabsorption and the subsequent bond breakings described in reactions 2 and 5 are simulated by propagations of selected wavepackets $\Psi_e(q_a,q_b,t)$ on the PES corresponding to the e excited states. The time evolution of the wavepackets is obtained by solving the time-dependent Schrödinger equation

$$i\hbar\frac{\partial}{\partial t}\Psi_e(q_a,q_b,t) = [T_{nu} + V_e]\Psi_e(q_a,q_b,t) \qquad (2)$$

with the initial condition

$$\Psi_e(q_a,q_b,t{=}0) = \mu_e\Phi_{gs,0,0}(q_a,q_b) \qquad (3)$$

where $\mu_e$ is the electronic transition moment between the ground state (gs) and the excited state e. $\Phi_{gs,0,0}(q_a,q_b)$ represents the two-dimensional vibrational ground state wave function of the electronic ground state evaluated through the Chebychev relaxation method.[52] The solution of the time-dependent Schrödinger eq 2 is obtained by the Chebychev propagation scheme with $\Delta t = 3$ fs.[53]

The absorption spectrum $\sigma_{tot(\omega)}$ is obtained by the Fourier transform of the total autocorrelation function $S_{tot}(t)$ summed over the individual autocorrelation functions corresponding to each excited state e

$$S_{tot}(t) = \sum_e \langle\Psi_e(0)|\Psi_e(t)\rangle \qquad (4)$$

The kinetic part of the Hamiltonian of the system, expressed in bond coordinates, is given by

$$T_{nu} = -\frac{\hbar^2}{2\mu_a}\frac{\partial^2}{\partial q_a^2} - \frac{\hbar^2}{2\mu_b}\frac{\partial^2}{\partial q_b^2} - \frac{\hbar^2\cos\theta}{m_c}\frac{\partial^2}{\partial q_a\partial q_b} \qquad (5)$$

where $\mu_a$ and $\mu_b$ are the reduced mass corresponding to the bonds $q_a$ and $q_b$ and $m_c$ the mass of the central atom (the angle $\theta$ is kept constant to its experimental value of 74.25°). Reaction probabilities are deduced by integration, over the whole reaction time, of the probability current density expressed as a function of coordinates $q_a$ and $q_b$[54]

$$\vec{J}(q_a,q_b,t) = \begin{pmatrix} J_a(q_a,q_b,t) \\ J_b(q_a,q_b,t) \end{pmatrix} \qquad (6)$$

where

$$J_a(q_a,q_b,t) = \frac{1}{\mu_a}\text{Re}\left(\Psi^*(q_a,q_b,t)\frac{\hbar}{i}\frac{\partial}{\partial q_a}\Psi(q_a,q_b,t)\right) +$$
$$\frac{\cos\theta}{m_c}\text{Re}\left(\Psi^*(q_a,q_b,t)\frac{\hbar}{i}\frac{\partial}{\partial q_b}\Psi(q_a,q_b,t)\right) \qquad (7)$$

and $J_b(q_a,q_b,t)$ being defined in the symmetric way.

The PES used in the simulation of the dynamics are generated by interpolation from ab initio points, with additional smoothing to avoid any obvious artifact such as shallow minima in the asymptotic domains. The propagations are based on representations of $\Psi_e(q_a,q_b,t)$ on two-dimensional grids corresponding to the reaction coordinates with the following parameters: $q_{a_i} =$

**Table 1.** CASPT2 and CCI Excitation Energies (in cm$^{-1}$) to the Lowest Excited States of $H_2Fe(CO)_4$ (This Work and Ref 25a)

| one electron excitation in the principal configuration | | CASPT2 | CASSCF/CCI |
|---|---|---|---|
| $a^1A_1 \rightarrow a^3B_1$ | $3d_{yz} \rightarrow \sigma_g^*$ | 32 803 | 30 092 |
| $a^1A_1 \rightarrow a^3A_1$ | $3d_{x^2-y^2} \rightarrow \sigma_g^*$ | 33 114 | 30 507 |
| $a^1A_1 \rightarrow a^3B_2$ | $3d_{x^2-y^2} \rightarrow \sigma_u^*$ | 33 479 | 33 026 |
| $a^1A_1 \rightarrow a^3A_2$ | $3d_{xz} \rightarrow \sigma_g^*$ | 33 804 | 33 826 |
| $a^1A_1 \rightarrow b^3A_2$ | $3d_{yz} \rightarrow \sigma_u^*$ | 35 485 | 36 910 |
| $a^1A_1 \rightarrow b^3B_1$ | $3d_{xz} \rightarrow \sigma_u^*$ | 38 032 | 40 550 |
| $a^1A_1 \rightarrow a^1B_1$ | $3d_{yz} \rightarrow \sigma_g^*$ | 38 713 | 38 520 |
| $a^1A_1 \rightarrow a^1B_2$ | $3d_{x^2-y^2} \rightarrow \sigma_u^*$ | 39 304 | 39 354 |
| $a^1A_1 \rightarrow a^1A_2$ | $3d_{xz} \rightarrow \sigma_g^*$ | 39 502 | 41 474 |
| $a^1A_1 \rightarrow b^3B_2$ | $\sigma_u \rightarrow \sigma_g^*$ | 41 316 | 62 028 |
| $a^1A_1 \rightarrow b^1A_1$ | $3d_{x^2-y^2} \rightarrow \sigma_g^*$ | 42 207 | 42 179 |
| $a^1A_1 \rightarrow b^1A_2$ | $3d_{yz} \rightarrow \sigma_u^*$ | 42 223 | 44 919 |
| $a^1A_1 \rightarrow b^1B_2$ | $\sigma_u \rightarrow \sigma_g^*$ | 47 922 | 68 667 |

**Table 2.** Electronic Dipole Transition Moments of the Lowest Singlet Excited States of $H_2Fe(CO)_4$

| | $_a^1A_1 \rightarrow _a^1B_1$ | $_a^1A_1 \rightarrow _a^1B_2$ | $_a^1A_1 \rightarrow _b^1A_1$ |
|---|---|---|---|
| $\mu$ (au) | 0.327 | 0.013 | 0.275 |

$q_{a_o} + (i-1)\Delta q_a$, $q_{a_o} = 0.5$ au, $\Delta q_a = 0.0670$ au with $1 \leq i \leq 128$ and $q_{b_j} = q_{b_o} + (j-1)\Delta q_b$, $q_{b_o} = 2$ au, $\Delta q_b = 0.315$ au with $1 \leq j \leq 256$.

## 3. Results and Discussion

**Theoretical Absorption Spectrum.** According to our recent CASSCF/CASPT2 calculations[25a] and to the present work the lowest excited states of $H_2Fe(CO)_4$ correspond to 3d $\rightarrow \sigma_g^*$ and 3d $\rightarrow \sigma_u^*$ excitations and range between 30 000 and 50 000 cm$^{-1}$ (Table 1). The first allowed transitions corresponding to $a^1A_1 \rightarrow a^1B_1$, $a^1A_1 \rightarrow a^1B_2$, and $a^1A_1 \rightarrow b^1A_1$ are calculated between 38 000 and 42 000 cm$^{-1}$ in the energy domain of the experimental absorption spectrum (34 500−41 500 cm$^{-1}$).[55] The calculated electronic dipole transition moments are reported in Table 2. The $a^1A_2$ (3d $\rightarrow \sigma_g^*$) excited state has been excluded from the simulation because the $a^1A_1 \rightarrow a^1A_2$ transition is symmetry forbidden. On the basis of a preliminary one-dimensional simulation it appears that the $a^1B_2$ (3d $\rightarrow \sigma_u^*$) state does not contribute significantly to the spectrum, due to a low value of the electronic transition dipole moment ($\mu = 0.013$ au).[56] Consequently, the main contributions to the absorption spectrum are the $a^1B_1$ ($b^1A'$ in $C_s$ symmetry) and $b^1A_1$ ($c^1A'$ in $C_s$ symmetry) excited states and correspond to 3d $\rightarrow \sigma_g^*$ excitations. The theoretical spectrum obtained by propagation of the $\Psi_{b^1A'}(q_a,q_b,t)$ and $\Psi_{c^1A'}(q_a,q_b,t)$ wavepackets on the $b^1A'$ and $c^1A'$ PES (the details of the simulation are described below) with the initial conditions given by eq 3 is shown in Figure 2. The spectrum is characterized by two broad absorption bands without any structure corresponding to the $a^1B_1$ and $b^1A_1$ states. The shape of the theoretical spectrum reflects the dissociative character of these two excited states. The $a^1B_1$ absorption at 36 700 cm$^{-1}$ agrees perfectly with the experimental maximum at 270 nm (37 040 cm$^{-1}$) for which there is no doubt experimentally.[55,57] The comparison with the experimental spectrum at higher energies is featureless, since the detection is close to the lower wavelength limit of the spectrometer. Consequently, an absorption around 40 500 cm$^{-1}$ corresponding to the $a^1A_1 \rightarrow b^1A_1$ transition cannot be excluded from the

(52) Kosloff, R.; Tal-Ezer, H. *Chem. Phys. Lett.* **1986**, *127*, 223.
(53) Kosloff, R. *J. Phys. Chem.* **1988**, *92*, 2087. Tal-Ezer, H.; Kosloff, R. *J. Chem. Phys.* **1984**, *81*, 3967. Kosloff, R. *Annu. Rev. Phys. Chem.* **1994**, *45*, 145.
(54) Katz, G.; Baer, R.; Kosloff, R. *Chem. Phys. Lett.* **1995**, *239*, 230.

(55) Sweany, R. L. Matrix Studies of Transition Metal Hydrides. In *Transition Metal Hydrides*; VCH Publishers: Dedieu, A., Ed.; 1991; pp 65−101.
(56) Heitz, M. C. Ph.D. Thesis, Strasbourg, France, 1996.
(57) Sweany, R. L. Private communication.
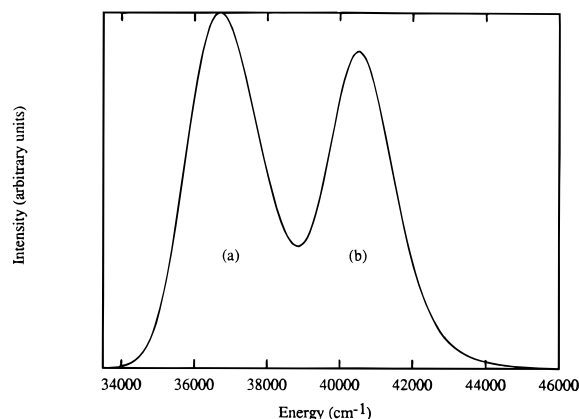
**Figure 2.** Simulated total absorption spectrum with contribution from two transitions $a^1A_1 \rightarrow a^1B_1$ (a) and $a^1A_1 \rightarrow b^1A_1$ (b).
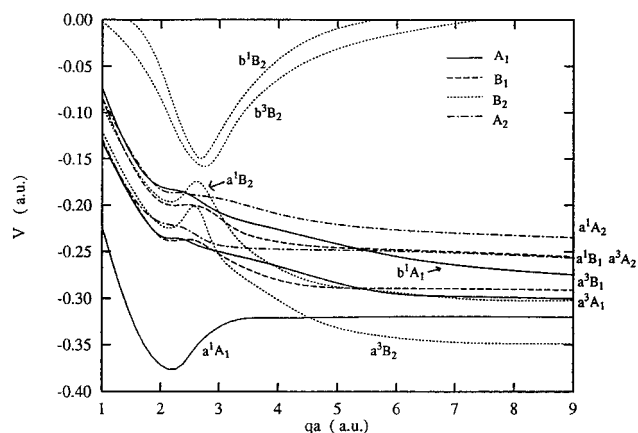


**Figure 3.** CASSCF/CCI potential energy curves along the $q_a$ = [Fe−H$_2$] bond elongation in H$_2$Fe(CO)$_4$.



**Figure 4.** CASSCF/CCI potential energy curves along the $q_b$ = [Fe−CO$_{ax}$] bond elongation in H$_2$Fe(CO)$_4$.

present simulation. The experimental excitation energy (254 nm or 39 400 cm$^{-1}$) necessary to induce elimination of molecular hydrogen from H$_2$Fe(CO)$_4$ (reaction 2) should populate the $a^1B_1$ and $b^1A_1$ excited states in the Franck−Condon approximation. According to the present simulation, the direct population of the $a^1B_2$ state corresponding to a 3d $\rightarrow$ $\sigma_u$* excitation and postulated as a key step in the mechanism of reaction 2 in a previous qualitative study[28] is less likely.

**Potential Energy Curves for the Molecular Hydrogen Elimination (Reaction 2).** The potential energy curves corresponding to the elimination of molecular hydrogen and calculated under $C_{2v}$ constraint are shown in Figure 3. Reaction 2 is calculated to be endothermic by 33.6 kcal/mol. According to the experimental data available in the literature,[58] the Fe−H bond energy in H$_2$Fe(CO)$_4$ ranges between 60 and 65 kcal/mol leading to an endothermicity comprised between 16 and 26 kcal/mol for reaction 2 which corresponds to the breaking of two iron−H bonds concurrently with the formation of one H−H bond. It is interesting to note that usually the calculated cost of this type of reaction is in the range 15−25 kcal/mol.[28] The complexity and the number of dissociative channels available from the low-lying excited states of H$_2$Fe(CO)$_4$ under the $C_{2v}$ constraint in the Franck−Condon region are illustrated by the shape of the potential energy curves in Figure 3. The potential energy curves corresponding to the $a^1B_1$ (3d$_{yz}$ $\rightarrow$ $\sigma_g$*) and $b^1A_1$ (3d$_{x^2-y^2}$ $\rightarrow$ $\sigma_g$*) excited states directly accessible through vertical transition from the $a^1A_1$ electronic ground state are dissociative. The potential energy curve corresponding to the $a^1B_2$ (3d$_{x^2-y^2}$ $\rightarrow$ $\sigma_u$*) excited state presents an energy barrier of the order of
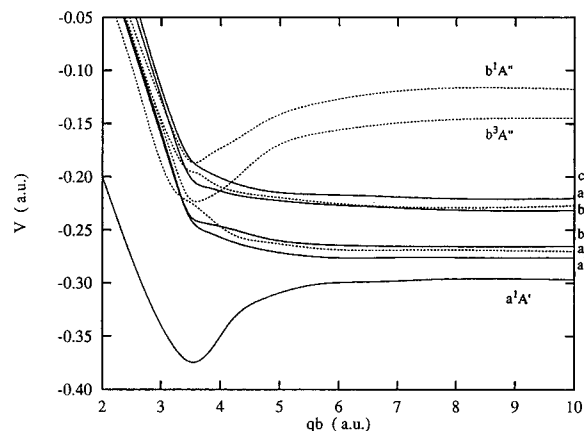
10.0 kcal/mol at the early stage of the reaction path due to an avoided crossing with the upper $b^1B_2$ ($\sigma_u \rightarrow \sigma_g$*) excited state. The PEC calculated in the present work do not differ drastically from the previous one obtained in a preliminary study based on less sophisticated calcultions.[28] In the energy domain of the absorption one may notice the presence of the dissociative $a^1A_2$ (3d$_{xz}$ $\rightarrow$ $\sigma_g$*) excited state which is not directly accessible through an allowed transition from the electronic ground state but which can play a role in the photodissociation of H$_2$Fe-(CO)$_4$ as soon as the $C_{2v}$ symmetry constraint is left (CO dissociation). The triplet PEC run more or less parallel to the corresponding singlet PEC and are dissociative. One may notice the presence of an energy barrier of the order of 14.0 kcal/mol on the $a^3B_2$ PEC leading to the primary products H$_2$ + Fe-(CO)$_4$ in their $^3B_2$ ground state, paramagnetic structure which has been determined experimentally.[32a]

**Potential Energy Curves for the Dissociation of a Carbonyl Ligand (Reaction 5).** The potential energy curves corresponding to the dissociation of a carbonyl ligand and calculated under $C_s$ constraint are shown in Figure 4. The PEC corresponding to the $a^1B_1$ ($b^1A'$) and $b^1A_1$ ($c^1A'$) excited states are weakly dissociative and nearly parrallel along the Fe−CO elongation. Under $C_s$ symmetry constraint the dissociative $a^1B_2$ ($a^1A''$) and the bound $a^1A_2$ ($b^1A''$) excited states are nearly degenerate and present an avoided crossing in the Franck−Condon region. The triplet PEC calculated along the Fe−CO elongation present the same features than the corresponding singlet PEC.

**One-Dimensional Simulation on Spin-Orbit Coupled Potentials.** The whole set of PEC shown in Figures 3 and 4 gives an illustration of the complexity of the reaction mechanisms in transition metal dihydrides due to the high density of excited states in the energy domain of the absorption spectrum and to the number of dissociative channels. In order to select the excited states playing a key role in the photodissociation and to determine the function of the low-lying triplet excited states, we have performed one-dimensional wavepacket propagations along the $q_a$ = [Fe−H$_2$] reaction coordinate on spin-orbit coupled potentials. Five excited states have been selected, the singlet $a^1B_1$, $a^1B_2$, and $b^1A_1$ states ranging in the absorption domain and the $a^3A_2$ and $a^3B_2$ states, both being close in energy to the singlets, the later leading to the primary products H$_2$ + Fe(CO)$_4$ in their ground state. The values of the spin-orbit coupling terms between the singlet and triplet excited states of H$_2$Fe(CO)$_4$ reported in Table 3 have been obtained through full-CI calculations restricted to ten valence electrons distributed in ten active orbitals ($\sigma_g$, $\sigma_u$, $\sigma_g$*, $\sigma_u$*, 3d, and the d which correlate them).[59] The spin-orbit interaction has been including at the
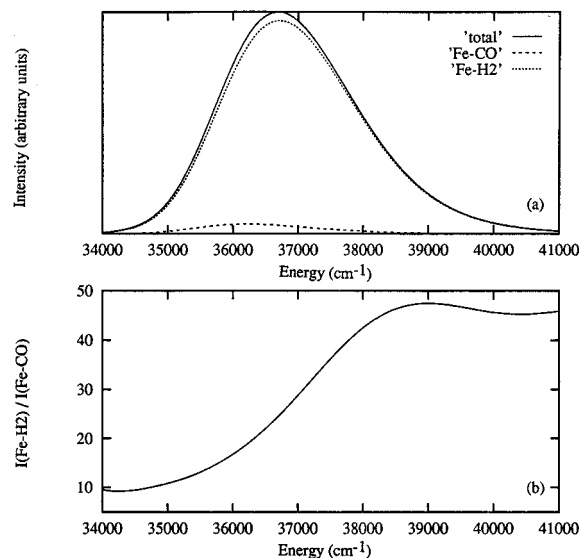
(58) (a) Pearson, R. G.; Mauermann, H. *J. Am. Chem. Soc.* **1982**, *104*, 500. (b) Pearson, R. G. *Chem. Rev.* **1985**, *85*, 41.

8274  *J. Am. Chem. Soc., Vol. 119, No. 35, 1997*

*Heitz and Daniel*

**Table 3.** Spin-Orbit Interaction (in cm$^{-1}$) between the Electronic Ground and Excited States of H$_2$Fe(CO)$_4$

|            | a$^3$B$_1$ | a$^3$A$_1$ | a$^3$B$_2$ | a$^3$A$_2$ | b$^3$A$_2$ | b$^3$B$_2$ |
|------------|------------|------------|------------|------------|------------|------------|
| a$^1$A$_1$ | 280        |            | 444        | 302        | 33         | 64         |
| a$^1$B$_1$ |            | 140        | 20         | 113        | 121        | 74         |
| a$^1$B$_2$ | 14         | 31         |            | 53         | 138        |            |
| b$^1$A$_1$ | 138        |            | 22         | 78         | 23         | 171        |

CI level as a one-electron effective operator (eq 1) with $Z_{eff} =$ 14.0, evaluated in the L−S coupling scheme from the iron atomic splitting in the $^5$D configuration. The time evolution of the wavepackets $\Psi_{b^1A_1}(q_a,t)$, $\Psi_{a^1B_1}(q_a,t)$, $\Psi_{a^1B_2}(q_a,t)$, $\Psi_{a^3B_2}(q_a,t)$, and $\Psi_{a^3A_2}(q_a,t)$ has been followed by propagation on the corresponding spin-orbit coupled potentials by solving sets of spin-orbit coupled time-dependent Schrödinger equations[60] using the values of Table 3 as coupling potentials.[59] From the time evolution of the $\Psi_{a^1B_2}(q_a,t)$ and $\Psi_{a^3A_2}(q_a,t)$ wavepackets on the spin-orbit coupled potentials $V_{a^1B_2}(q_a)$ and $V_{a^3A_2}(q_a)$ one may extract the probabilities for observing either the reaction H$_2$-Fe(CO)$_4 \rightarrow$ H$_2$ + Fe(CO)$_4$ (a$^1$B$_2$) or the reaction H$_2$Fe(CO)$_4 \rightarrow$ H$_2$ + Fe(CO)$_4$ (a$^3$A$_2$) as a function of time. An indirect dissociation of H$_2$ through tunnelling is observed on the a$^1$B$_2$ potential with a probability of 2% in 1 ps. The a$^1$B$_2 \rightarrow$ a$^3$A$_2$ intersystem crossing probability is 0.35% in 1 ps. The results of the one-dimensional simulation along the Fe−H$_2$ bond elongation can be summarized as follows: (i) the direct dissociation of molecular hydrogen on the a$^1$B$_1$ and b$^1$A$_1$ potentials is total and ultrafast (a few femtoseconds) leading to the H$_2$ + Fe(CO)$_4$ primary products in excited configurations; (iii) the indirect dissociation through the a$^1$B$_2$ is not competitive with the direct ultrafast dissociation toward H$_2$ + Fe(CO)$_4$ (a$^1$B$_1$, b$^1$A$_1$); and (iii) the nonradiationless transitions to the low-lying triplet states occur in a picosecond time scale and have a rather low probability.

**Simulation of the Dynamics on Two-Dimensional Potentials.** On the basis of the results reported above, the two low-lying a$^1$B$_1$ (b$^1$A$'$ in $C_s$ symmetry) and b$^1$A$_1$ (c$^1$A$'$ in $C_s$ symmetry) excited states, directly accessible under UV irradiation and contributing mainly to the absorption spectrum of H$_2$-Fe(CO)$_4$, have been used in the two-dimensional simulation. The time evolution of the system on these excited states has been followed by propagation of the $\Psi_{b^1A'}(q_a,q_b,t)$ and $\Psi_{c^1A'}(q_a,q_b,t)$ wavepackets on the $V_{b^1A'}(q_a,q_b)$ and $V_{c^1A'}(q_a,q_b)$ potentials under the $C_s$ symmetry constraint. The kinetic coupling between the two potentials has not been taken into account in the present simulation. After the initial a$^1$A$'$ (a$^1$A$_1$ in $C_{2v}$ symmetry) $\rightarrow$ b$^1$A$'$ (a$^1$B$_1$ in $C_{2v}$ symmetry) transition, in a very short time scale (15 fs) the wavepacket evoluates to the dissociation channel corresponding to the H$_2$ elimination (Figure 5). After 30 fs one observes a splitting of the initial wavepacket in two parts: the main fraction leads to the primary products H$_2$ + Fe(CO)$_4$ (b$^1$A$'$) in 40 fs, the remaining part dissociates to the carbonyl loss primary products in a time scale of the order of 100 fs. The two concurrent primary reactions (reactions 2 and 5) are observed on the $V_{b^1A'}(q_a,q_b)$ potential originating in the a$^1$B$_1$ (3d$_{yz} \rightarrow \sigma_g^*$) excited state. The probability of the minor reaction, namely the dissociation of a CO ligand, deduced by integration over the whole reaction time of the probability current density (eqs 6 and 7) is of the order of 4%. The branching ratio between the two concurrent reactions $\alpha =$ H$_2$-Fe(CO)$_4$* (a$^1$B1) $\rightarrow$ H$_2$ + Fe(CO)$_4$ and $\beta =$ H$_2$Fe(CO)$_4$*(a$^1$B$_1$) $\rightarrow$ H$_2$Fe(CO)$_3$ + CO has been determined as a function of the absorption frequency on the basis of the partial absorption

(59) Cardoen, W.; Ribbing, C.; Heitz, M. C.; Daniel, C. To be published.
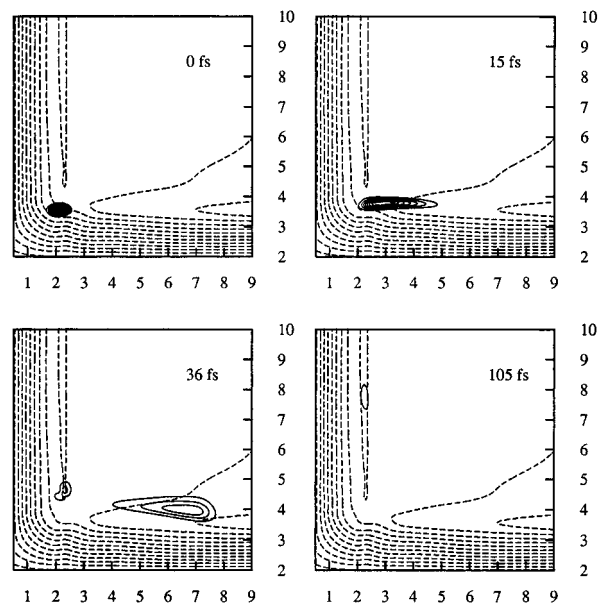


**Figure 5.** Time evolution of the $|\Psi_{bA'}^1(q_a,q_b,t)|$ wavepacket on the $V(A_b^{1'})$ potential.



**Figure 6.** Total $\sigma_{tot}(\omega)$ (solid line) and partial $\sigma_\alpha(\omega)$ (dotted line) and $\sigma_\beta(\omega)$ (dashed line) A$_a^{1'} \rightarrow$ A$_b^{1'}$ absorption spectra with contributions from two competing products channels $\alpha \equiv$ H$_2$Fe(CO)$_4^* \rightarrow$ H$_2$ + Fe(CO)$_4$ and $\beta \equiv$ H$_2$Fe(CO)$_4^* \rightarrow$ H$_2$Fe(CO)$_3$ + CO (a) branching ratio [$\alpha,\omega$]/[$\beta,\omega$] = $\sigma_\alpha(\omega)/\sigma_\beta(\omega)$ as a function of the absorption frequency $\omega$.

spectra (Figure 6). The elimination of molecular hydrogen is the major process overall the absorption region and the probability of this primary reaction increases with the wavelength of irradiation.

The time evolution of the $\Psi_{c^1A'}(q_a,q_b,t)$ wavepacket on the $V_{c^1A'}(q_a,q_b)$ potential, originated in the b$^1$A$_1$ (3d$_{x^2-y^2} \rightarrow \sigma_g^*$) excited state of H$_2$Fe(CO)$_4$, has been followed as a function of the time. Despite the dissociative character of this potential in both directions, the Fe−H$_2$ and the Fe−CO elongations (Figures 3 and 4), the initial wavepacket turns entirely into the channel corresponding to the elimination of H$_2$ in a total ultrafast reaction in less than 40 fs.

**Reverse Oxidative Addition.** In a previous qualitative analysis of the reverse oxidative addition,[28] observed under visible irradiation at low temperature,[16] we had proposed three possible hypotheses to explain the mechanism of this reaction.

One of these hypotheses was based on spin-orbit interactions considerations. This hypothesis is supported by the present work. Indeed, on the basis of the results reported in Table 3, the spin-orbit coupling between the $a^1A_1$ electronic ground state and the $a^3B_2$ excited state which correlates with the primary products $H_2 + Fe(CO)_4$ in their ground states has a value of $444$ cm$^{-1}$ at the equilibrium geometry. Moreover the shape of the corresponding PEC (Figure 3) presents a crossing around a Fe$-$H$_2$ distance of 3.0 Å. Even if the spin-orbit interaction has not been evaluated as a function of the reaction coordinate, according to recent simulations of intersystem crossing processes in organometallics,[60] this value is large enough to induce radiationless transitions.

**Conclusion**

Electronic ground and excited states CASSCF/CCI potential energy surfaces have been calculated as a function of two coordinates $q_a$ and $q_b$, corresponding to some primary photo-dissociation pathways of $H_2Fe(CO)_4$, namely the elimination of $H_2$ and the dissociation of an axial carbonyl ligand. The number and the diversity of excited states situated in a rather limited domain of energy (less than 2.0 eV in the UV region) leads to a complicated network of dissociative or weakly bound triplet and singlet curves characterized by several energy barriers due to avoided crossings. This theoretical work illustrates the complexity of the photodissociation mechanisms operating in organometallics and points to the limits of a qualitative study which would be based on molecular orbitals diagrams coupled with an analysis in terms of bonding and antibonding character. Indeed, the nature of the states involved in the photochemistry is modified all along the reactions paths, mainly due to the evolution of the three centers interaction which characterizes the metal dihydrides. As a consequence, a multiconfigurational approach is mandatory to describe correctly the photodissociation pathways. On the basis of a one-dimensional simulation of the dynamics on spin-orbit coupled potentials, we have shown that intersystem crossing processes in this molecule are not competitive with the direct dissociations which occur in less

than 100 fs. The simulation of the photodissociation dynamics in two dimensions leads to the following conclusions: (i) the elimination of $H_2$ is the major process under irradiation in the UV domain of energy; (ii) the time scale of the photoelimination of $H_2$ is of the order of a few tens of femtoseconds; (iii) the dissociation of the axial CO ligand is a minor process occuring within 100 fs; (iv) among the number of excited states present in the UV region, only two singlet excited states contribute significantly to the absorption spectrum. These conclusions agree rather well with the experimental findings in low temperature matrices experiments, namely an exclusive elimination of $H_2$ in $H_2Fe(CO)_4$ and an absorption band around 270 nm. Moreover, a time scale of 100 fs for the carbonyl loss is in accord with the recent results of time-resolved experiments, using ultrafast laser pulses, reported for transition metal carbonyls in gas phase.[61] The present work which reports the complete simulation of the photodissociation dynamics of $H_2$-$Fe(CO)_4$ including all excited states in a two-dimensional scheme has enabled us to propose a semiquantitative understanding of the mechanism. The low efficiency of intersystem crossing processes and the main features of the absorption spectrum indicate that only a few excited states participate to the whole photochemical behavior of the molecule. The time scales of the direct dissociations (less than 100 fs) justify the limitation of degrees of freedoms to two reaction coordinates, at least in a first approximation. However, a more detailed investigation of the potentials could display the importance of other degrees of freedoms or point to other reaction paths. This work, based on Gradient CASSCF calculations, is in progress.

**Supporting Information Available:** Tables of CASSCF/CCI energies as a function of the coordinates $q_a =$ [Fe$-$H$_2$] and $q_b =$ [Fe$-$Coax] (2 pages). See any current masthead page for ordering and Internet access instructions.

(60) Daniel, C.; Heitz, M. C.; Ribbing, C.; Manz, J. *J. Chem. Phys.* **1995**, *102*(2), 905. Heitz, M. C.; Ribbing, C. Daniel, C. *J. Chem. Phys.* **1997**, *106(4)*, 1421.

(61) Kim, S. K.; Pedersen, S.; Zewail, A. H. *Chem. Phys. Lett.* **1995**, *233*, 500. Banares, L.; Baumert, T.; Bergt, M.; Kiefer, B.; Gerber, G. *Chem. Phys. Lett.* **1997**, *267 (1−2)*, 141.

JA9643127